

# EVALUATION OF NON-LINEAR COMBINATIONS OF RESCALED REASSIGNED SPECTROGRAMS

*Maria Hansson-Sandsten* \*

Lund University  
Mathematical Statistics,  
Centre for Mathematical Sciences  
Box 118, SE-221 00 Lund, Sweden

## ABSTRACT

The reassignment technique is used to increase the localization for signals that have closely located time-frequency components. For Gaussian components the reassignment based on an optimal (matched) window spectrogram will result in a single point where all mass is located. For non-optimal windows, the reassignment procedure can be optimally rescaled to fulfill the single point mass location. Non-linear combinations of spectrograms for different window lengths have previously been suggested, [1], and in this paper an evaluation is made of the performance for different non-linear combinations of optimally rescaled reassigned spectrograms.

*Index Terms*— time-frequency, reassignment, localization, Hermite function

## 1. INTRODUCTION

The idea of reassignment is to keep the localization of a single component by reassigning mass to the center of gravity, [2, 3]. For multi-component signals, the reassignment improves the readability as the cross-terms are reduced by a smoothing of the specific distribution and the reassignment then squeezes the signals terms. However, the reassignment technique can be sensitive to noise disturbances and reassigned multitaper spectrograms has also been proposed for noise reduction, [4]. Recently, the theoretical expressions for the reassigned Gabor spectrograms of Hermite functions have been derived in [5, 6]. Applying the optimal length first Hermite function as window followed by a calculation of a reassigned spectrogram will result in a single point where all the mass of the signal is localized. The reassignment procedure is, however, sensitive when several components are closely located. This limitation is of course connected to the resolution of the spectrogram. Depending on if the time-frequency components are closest in the time- or frequency direction, it could be desirable to adjust the window length to either longer or shorter. The reassignment of the resulting spectrogram will

then not be perfectly localized to a single point. The adjustment needed for the use of a longer or shorter window can however be calculated and applied in the reassignment procedure. It is then possible to receive a number of perfectly localized reassigned spectrograms using different window lengths. A first attempt of this was proposed in [7].

In [1], ideas of combining spectrograms of different window lengths in some optimal ways were presented. The Minimum Mean Cross-Entropy (MMCE) and the Minimax Cross-Entropy solutions were shown to result in the geometrical mean and the point-wise minimum power of the set of spectrograms respectively. Based on this, an evaluation of different optimal combinations of reassigned spectra is made in this paper. The evaluation is limited to the combination of one short-length and one long-length spectrogram and the resulting combination in the arithmetic mean, geometric mean as well as the point-wise minimum power is evaluated for different pairs of window lengths.

In section 2, the novel technique of rescaled reassigned spectrogram of a Hermite function windowed Gaussian signal is presented. Section 3 evaluates the performance of the proposed technique in the non-linear combinations of reassigned spectrograms. Section 4 concludes the paper.

## 2. REASSIGNED SPECTROGRAMS

A Gaussian windowed constant frequency signal

$$x(t) = g(t - t_0)e^{-i\omega_0 t}, \quad (1)$$

where the unit-energy Gaussian function is

$$g(t) = \pi^{-\frac{1}{4}} e^{-\frac{1}{2}t^2}, \quad -\infty < t < \infty \quad (2)$$

is often used to model a short non-stationary signal. The quadratic class of distributions obey time-frequency shift-invariance  $S_x(t - t_0, \omega - \omega_0) = S_g(t, \omega)$ , meaning that the further analysis can be restricted to  $x(t) = g(t)$ . The magnitude of the short-time Fourier transform for the signal in

---

\*Thanks to the Swedish Research Council and eSENCE for funding

Eq. (2) applying a Hermite function window is, [5],

$$M_g^{hk}(t, \omega) = \frac{1}{\sqrt{2^{k-1}(k-1)!}} (t^2 + \omega^2)^{\frac{(k-1)}{2}} e^{-\frac{1}{4}(t^2 + \omega^2)}, \quad (3)$$

and the spectrogram is found as

$$SP_g^{hk}(t, \omega) = |M_g^{hk}(t, \omega)|^2. \quad (4)$$

The corresponding reassigned spectrogram is

$$\begin{aligned} ReSP_g^{hk}(t, \omega) &= \\ &= \frac{1}{2\pi} \iint_{-\infty}^{\infty} SP_g^{hk}(s, \xi) \delta(t - \hat{t}(s, \xi), \omega - \hat{\omega}(s, \xi)) ds d\xi, \end{aligned} \quad (5)$$

where for spectrograms based on the Hermite function windows of a Gaussian signal the more recent formulation, [6], can be used, i.e.,

$$\begin{aligned} \hat{t}(t, \omega) &= t + \frac{\partial}{\partial t} \log M_g^{hk}(t, \omega) \\ \hat{\omega}(t, \omega) &= \omega + \frac{\partial}{\partial \omega} \log M_g^{hk}(t, \omega). \end{aligned} \quad (6)$$

Only the first Hermite function leads to perfect localization when the reassignment technique is applied. For all Hermite functions  $k > 1$ , the reassigned spectrograms will be circles, [5]. Therefore we restrict to the first Hermite function for further use in the reassignment procedure. For the first Hermite function

$$h(t) = \frac{1}{\sqrt{\sqrt{2\pi}}} e^{-\frac{t^2}{2}},$$

circular symmetry gives the spectrogram ( $SP$ ),

$$SP_g^h(t, \omega) = e^{-\frac{1}{2}(t^2 + \omega^2)}. \quad (7)$$

Using the reassignment operators, Eq. (6), [5], the perfect localized reassigned spectrogram is given by Eq. (5), ( $ReSP$ ).

## 2.1. Combinations of rescaled reassigned spectrograms

Another window length is given by the rescaling the time axis of the first Hermite function with a factor  $c$ , i.e.,

$$h_c(t) = \frac{1}{\sqrt{c\sqrt{2\pi}}} e^{-\frac{t^2}{2c^2}},$$

and we calculate the corresponding spectrogram as

$$\begin{aligned} SP_g^{hc}(t, \omega) &= \frac{1}{c\sqrt{2\pi}} \left| \int_{-\infty}^{\infty} e^{-\frac{s^2}{2c^2}} e^{-\frac{(s-t)^2}{2}} e^{-i\omega s} ds \right|^2 \\ &= \frac{1}{c\sqrt{2\pi}} e^{-t^2} \left| \int_{-\infty}^{\infty} e^{-\frac{(c^2+1)}{2c^2}s^2} e^{(t-i\omega)s} ds \right|^2 \\ &= \frac{\sqrt{2}c}{c^2+1} e^{-\frac{1}{2}\left(\frac{2}{c^2+1}t^2 + \frac{2c^2}{c^2+1}\omega^2\right)}. \end{aligned} \quad (8)$$

The resulting scaling of the time-axis is

$$c_t = \frac{(c^2 + 1)}{2}, \quad (9)$$

and the frequency axis

$$c_\omega = \frac{(c^2 + 1)}{2c^2}. \quad (10)$$

As we now have knowledge of the actual error in the time-frequency domain introduced by the scaled Hermite function, the reassignment procedure can be compensated accordingly,

$$\begin{aligned} ReSP_g^{hc}(t, \omega) &= \\ &= \frac{1}{2\pi} \iint_{-\infty}^{\infty} SP_g^{hc}(s, \xi) \delta(t - c_t \hat{t}(s, \xi), \omega - c_\omega \hat{\omega}(s, \xi)) ds d\xi, \end{aligned} \quad (11)$$

which will give us a perfectly localized spectrum using the window length scaled by  $c$ . In this paper, the evaluation is limited to the combination of two spectrograms with different window lengths, one with the scaling factor  $c$  and one with the scaling factor  $1/c$ . These two spectrograms are combined in different ways and is also compared to the results of the similar combinations of the usual spectrograms. The usual arithmetic means are calculated as

$$\begin{aligned} SP_{ari}(t, \omega) &= (SP_g^{hc}(t, \omega) + SP_g^{h1/c}(t, \omega))/2 \\ ReSP_{ari}(t, \omega) &= (ReSP_g^{hc}(t, \omega) + ReSP_g^{h1/c}(t, \omega))/2, \end{aligned}$$

and the geometric means are calculated as

$$\begin{aligned} SP_{geo}(t, \omega) &= \sqrt{SP_g^{hc}(t, \omega) \cdot SP_g^{h1/c}(t, \omega)} \\ ReSP_{geo}(t, \omega) &= \sqrt{ReSP_g^{hc}(t, \omega) \cdot ReSP_g^{h1/c}(t, \omega)}, \end{aligned}$$

giving the MMCE solution, [1]. The minimax cross-entropy solution, found in the same paper, is obtained as

$$\begin{aligned} SP_{min}(t, \omega) &= \min\{SP_g^{hc}(t, \omega) SP_g^{h1/c}(t, \omega)\} \\ ReSP_{min}(t, \omega) &= \min\{ReSP_g^{hc}(t, \omega) ReSP_g^{h1/c}(t, \omega)\}, \end{aligned}$$

## 3. SIMULATIONS

The simulated signal consists of a number of equal amplitude complex-valued Gaussian components, at different time- and frequency locations. Each Gaussian component length is 50 samples, measured as the number of samples increasing 99% of the maximum power. The total signal length is 600 samples and the FFT-length in the calculations is 1024. In Figure 1, examples of the performance of all the different methods can be seen. The signal is in this case two Gaussian components with the time distance  $\Delta t = 34$  samples and  $\Delta\omega = 2\pi\Delta f = 2\pi 0.03$ . The increased readability of the reassignment technique is notable in Figure 1a) and b), where examples of the resulting time-frequency representations of the usual spectrogram ( $SP$ ) with the optimal length

window ( $c = 1$ ) and the corresponding reassigned spectrogram ( $ReSP$ ) are shown, (dB-based colour scale). For the combined window methods, the scaling parameter  $c = 0.2$  is used, which will give the resulting combination of two spectrograms with one short window and one long window. The short window  $1/c = 5$  is approximately 20 samples and the long window with  $c = 0.2$  has a length around 512 samples. For the spectrogram based methods ( $SP$ ,  $SP_{ari}$ ,  $SP_{geo}$  and  $SP_{min}$ ) it is difficult to see that the signal consists of two components. For the reassigned spectrogram based methods, all plots, except perhaps  $ReSP_{ari}$ , show the two components. The  $ReSP_{geo}$  and  $ReSP_{min}$  are however better in localization than the  $ReSP$ . As the focus is on time-frequency concentration, the evaluation is performed based on the Rényi entropy of order  $\alpha$ ,

$$R_\alpha(SP) = \frac{1}{1-\alpha} \log_2 \int_{t_0}^{t_1} \int_{\omega_0}^{\omega_1} (SP(t, \omega))^\alpha dt d\omega, \quad (12)$$

for  $\alpha > 0$ , and any energy normalized time-frequency distribution  $SP(t, \omega)$ , [4, 8, 9]. The Rényi entropy is calculated for the often used  $\alpha = 3$ , [9], and  $t_0 = 128$ ,  $t_1 = 600 - 128 = 472$ ,  $\omega_0 = 2\pi f_0 = 0$  and  $\omega_1 = 2\pi f_1 = 2\pi \cdot 0.25$  in all cases. The resulting Rényi entropies for the four spectrogram based examples are  $R_3(SP) = 11.6$ ,  $R_3(SP_{ari}) = 13.4$ ,  $R_3(SP_{geo}) = 12.3$  and  $R_3(SP_{min}) = 11.5$ , and for the four reassigned spectrogram based examples  $R_3(ReSP) = 4.14$ ,  $R_3(ReSP_{ari}) = 4.03$ , and the lowest values given by  $R_3(ReSP_{geo}) = 3.21$  and  $R_3(ReSP_{min}) = 3.57$ . The values show that the visual performance is mirrored in the Rényi entropy values.

The first evaluation is made for two Gaussian components where one is fixed at  $t = 256$  and  $f = 0.1$  and one located at larger values of  $t$  and  $f$  moving in time and frequency. The evaluation is made for different values of the scaling parameter  $c$  ranging between 0.2 and 0.995. The scaling  $c = 0.995$ ,  $1/c = 1.005$ , will give two spectrograms that are very similar to the optimal one ( $c = 1$ ), although not identical. The Rényi entropies are calculated and the minimum value as a function of  $c$  is extracted for all the methods. For the spectrogram methods, the resulting Rényi entropies for the spectrogram ( $SP$ ) is close to  $R_3(SP) = 11.8$  for all time-frequency distances. The minimum Rényi entropies for the  $SP_{ari}$  and  $SP_{geo}$  is found to be the same value and the corresponding  $c_{min} = 0.995$  showing that there is no increased localization performance using the arithmetic and geometric means for un-disturbed signals. For the  $SP_{min}$  method, however, the resulting minimum Rényi entropies are around  $R_3(SP_{min}) = 11.4$  given by the value  $c_{min} = 0.5$  for all time-frequency distances, showing an increased performance using the scaling  $c = 0.5$  and  $1/c = 2$  for the two windows.

For the reassigned methods, the minimum Rényi entropies are depicted in Figure 2. All methods give the smallest possible Rényi entropy equal to one (for a sum of two equal com-

ponents), when the two components are at sufficiently large time-frequency distance. The curves of  $ReSP_{ari}$  and  $ReSP$  coincide for almost all values, explained by that the minimum Rényi entropies of  $ReSP_{ari}$  are given for values of  $c$  close to one, and we can conclude that the arithmetic mean is not useful for the reassigned spectra for un-disturbed signals. The minimum Rényi entropies for  $ReSP_{geo}$  and  $ReSP_{min}$ , given from  $c_{min} = 0.2$ , are however significantly smaller than for the  $ReSP$  for the values around  $\Delta t = 55$  and  $\Delta f = 0.045$  showing the increased precision of the proposed methods compared to the  $ReSP$ .

The components of Gaussian signals are disturbed by white Gaussian noise where the SNR is defined as the average power of the signal components divided by the noise variance,

$$\text{SNR} = 10 \log_{10} \frac{\frac{1}{T} \int_T x^2(t)}{\sigma_{noise}^2}. \quad (13)$$

The parameter  $T$  is defined as the time interval where we find at least the level of 99% of the maximum power of the signal. In the first case, we have two Gaussian components located with  $\Delta t = 34$  and  $\Delta f = 0.03$ , with the same locations as in Figure 1. The length of the sum of the components is  $T = 90$ , and the resulting SNR=30 dB, Figure 3a). The averaged Rényi entropies of 20 realizations are shown in Figure 4 as a function of the scaling parameter  $c$ . The smallest Rényi entropy is given by  $c = 0.5$  for the  $SP_{min}$  of the spectrogram based methods, Figure 4a). The  $SP_{geo}$  and  $SP_{ari}$  are not superior to the optimal spectrogram  $SP$ . For the reassigned methods, similarly as for the noise-free case, we can find values of  $c$  where the  $ReSP_{geo}$  and  $ReSP_{min}$  give smaller Rényi entropy than the usual optimal  $ReSP$ . The optimal value of  $c$ , ( $c = 0.6 - 0.9$ ) is however larger than in the undisturbed case, ( $c = 0.2$ ), which indicates that the parameter choice is sensitive to noise. For all spectrogram based methods the standard deviation of the 20 Rényi entropies are very small but the mean value  $\pm$  one standard deviation is depicted with crosses for the  $SP$  and the  $SP_{min}$  anyway in Figure 4a). For the reassigned methods however, the standard deviation is much larger which can be seen in Figure 4b) where this is indicated for the  $ReSP$  and for the  $ReSP_{min}$ . The other methods have similar behavior.

For the case of low SNR=10 dB, there are three Gaussian components located with  $\Delta t = 34$  and  $\Delta f = 0.03$  between the first a second one (similar as before) and one additional component with  $\Delta t = 34$  and  $\Delta f = 0.03$  between the second and third one. The signal power of the SNR is calculated based on the total power of the Gaussian components divided by  $T = 120$ , Figure 3b). The average Rényi entropies of 20 realizations are shown in Figure 5 where the results of the spectrogram based methods show similar behavior as for the previous simulation, (although located at a higher values). The standard deviation has also increased compared to the previous example. For the reassigned methods, a slightly changed performance is seen, the  $ReSP_{geo}$  and  $ReSP_{min}$

still give smaller Rényi entropies than the usual  $ReSP$ , although now the optimal parameter choice seems to be  $c$  close to one, again indicating the parameter sensitivity of noise.

#### 4. CONCLUSIONS

The spectrograms and rescaled reassigned spectrograms are combined in different linear and non-linear estimates, where the localization performance is evaluated using the Rényi entropy measure. The results show that the point-wise minimum power estimate and geometric mean results in increased localization compared to the reassigned optimal spectrogram. The parameter choice (window lengths) is however sensitive to noise disturbances.

#### REFERENCES

- [1] P. Loughlin, J. Pitton, and B. Hannaford, "Approximating time-frequency density functions via optimal combinations of spectrograms," *IEEE Signal Processing Letters*, vol. 1, no. 12, pp. 199–202, December 1994.
- [2] K. Kodera, C. de Villedary, and R. Gendrin, "A new method for the numerical analysis of nonstationary signals," *Physics of the Earth & Planetary Interiors*, vol. 12, pp. 142–150, 1976.
- [3] F. Auger and P. Flandrin, "Improving the readability of time-frequency and time-scale representations by the reassignment method," *IEEE Trans. on Signal Processing*, vol. 43, pp. 1068–1089, May 1995.
- [4] J. Xiao and P. Flandrin, "Multitaper time-frequency reassignment for nonstationary spectrum estimation and chirp enhancement," *IEEE Trans. on Signal Processing*, vol. 55, no. 6, pp. 2851–2860, June 2007.
- [5] P. Flandrin, "A note on reassigned Gabor spectrograms of hermite functions," *J Fourier Analysis and Applications*, vol. 19, no. 2, pp. 285–295, 2013, doi 10.1007/s00041-012-9253-2.
- [6] F. Auger, E. Chassande-Mottin, and P. Flandrin, "On phase-magnitude relationships in the short-time fourier transform," *IEEE Signal Processing Letters*, vol. 19, no. 5, pp. 267–270, May 2012.
- [7] M. Hansson-Sandsten and J. Starkhammar, "A refined time-frequency reassignment technique applied to dolphin echo-location signals," in *Proc. of the ICASSP*, Florence, Italy, 2014, IEEE.
- [8] S. Aviyente and W. J. Williams, "Minimum entropy time-frequency distributions," *IEEE Signal Processing Letters*, vol. 12, pp. 37–40, January 2005.
- [9] R. G. Baraniuk, P. Flandrin, A. J. E. M. Janssen, and O. J. J. Michel, "Measuring time-frequency information content using Rényi entropies," *IEEE Trans. on Information Theory*, vol. 47, no. 4, pp. 1391–1409, May 2001.

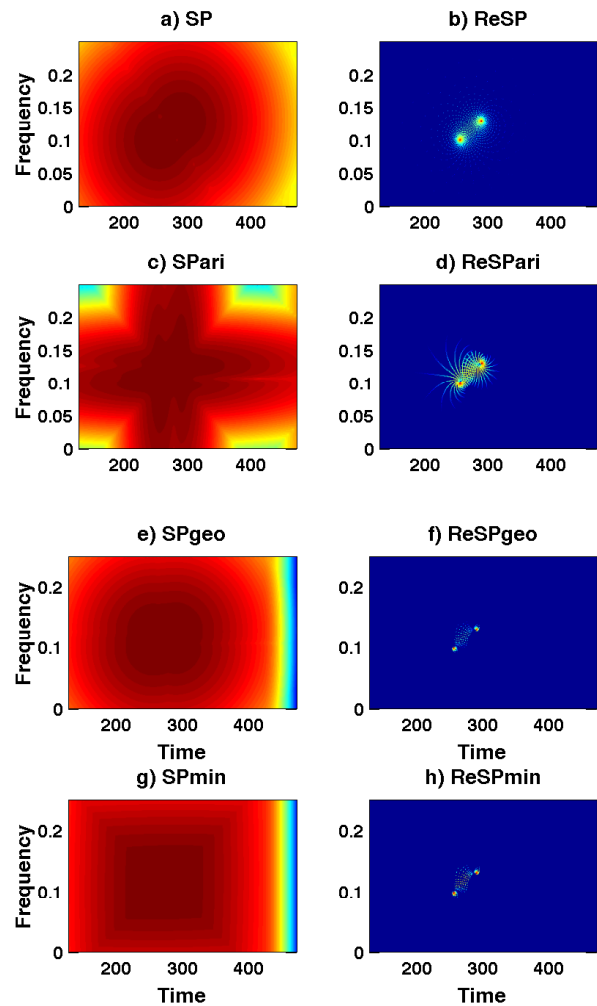


**Fig. 1.** Example of the time-frequency representations for some of the methods applied to estimation of two closely located Gaussian signals.

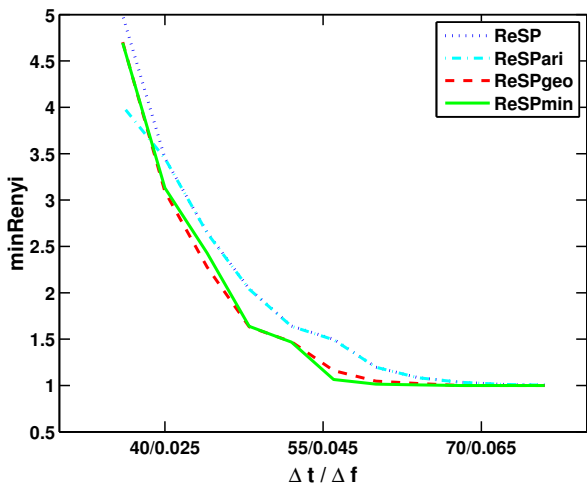


**Fig. 2.** The minimum Rényi entropy for the different re-assigned methods for two Gaussian components of different time-frequency distances  $\Delta t$  and  $\Delta f$ .

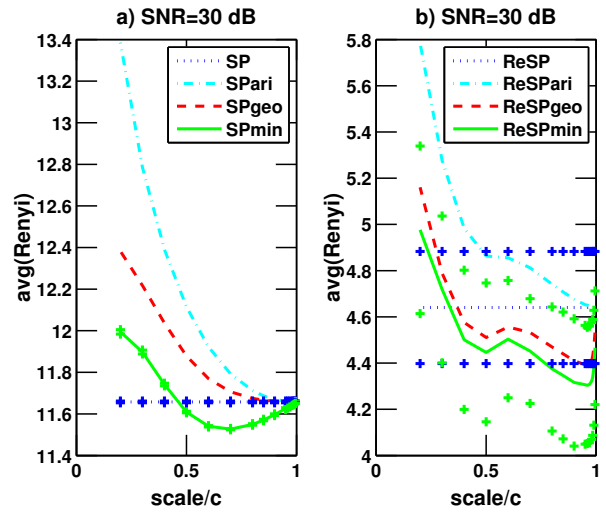


**Fig. 4.** The averaged Rényi entropies for the different methods for three Gaussian components disturbed by white noise with SNR=30 dB.

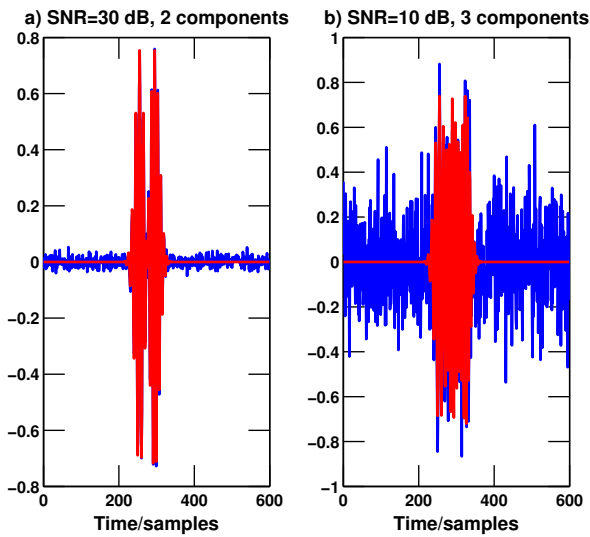


**Fig. 3.** a) Case 1: The two-component data with small disturbance, SNR=30 dB; b) Case 2: The three-component data with larger disturbance, SNR=10 dB.

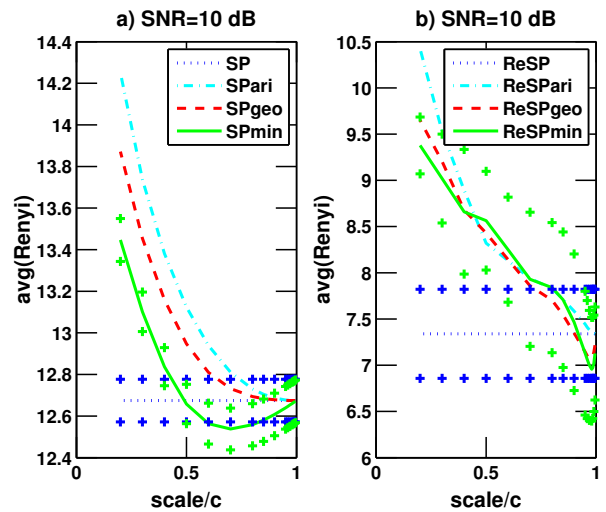


**Fig. 5.** The averaged Rényi entropies for the different methods for three Gaussian components disturbed by white noise with SNR=10 dB.